REPORT DOCUMENTATION PAGE

Form Approved
OMB No. 0704-0188

1. AGENCY USE ONLY (Leave blank)	2. REPORT DATE	3. REPORT TYPE AND DATES COVERED

4. TITLE AND SUBTITLE
Cylinder-Averaged Histories of Nitrogen Oxide in a D.I. Diesel With Simulated Turbocharging

5. FUNDING NUMBERS
DAAL03-92-G-0122

6. AUTHOR(S)
Ron Donahue, Gary Borman, Glenn Bower

7. PERFORMING ORGANIZATION NAME(S) AND ADDRESS(ES)
University of Wisconsin-Madison
Engine Research Center
1500 Johnson Drive
Madison, WI 53706

8. PERFORMING ORGANIZATION REPORT NUMBER

9. SPONSORING/MONITORING AGENCY NAME(S) AND ADDRESS(ES)
U. S. Army Research Office
P. O. Box 12211
Research Triangle Park, NC 27709-2211

10. SPONSORING/MONITORING AGENCY REPORT NUMBER
ARO 30340.25-EG-URI

11. SUPPLEMENTARY NOTES
The view, opinions and/or findings contained in this report are those of the author(s) and should not be construed as an official Department of the Army position, policy, or decision, unless so designated by other documentation.

12a. DISTRIBUTION/AVAILABILITY STATEMENT
Approved for public release; distribution unlimited.

12b. DISTRIBUTION CODE

13. ABSTRACT (Maximum 200 words)

An experimental study was conducted using the dumping technique (total cylinder sampling) to produce cylinder mass-averaged nitric oxide histories.

Data were taken using a four stroke diesel research engine employing a quiescent chamber, high pressure direct injection fuel system, and simulated turbocharging. Two fuels were used to determine fuel cetane number effects. Two loads were run, one at an equivalence ratio of 0.5 and the other at a ratio of 0.3. The engine speed was held constant at 1500 rpm. Under the turbocharged and retarded timing conditions of this study, nitric oxide was produced up to the point of about 85% mass burned.

Two different models were used to simulate the engine run conditions: the phenomenological Hiroyasu spray-combustion model, and the three dimensional, U.W.-ERC modified KIVA-II computational fluid dynamic code. Both of the models predicted the correct nitric oxide trend. Although the modified KIVA-II combustion model using Zeldovich kinetics correctly predicted the shapes of the nitric oxide histories, it did not predict the exhaust concentrations without arbitrary adjustment based on experimental values.

14. SUBJECT TERMS	15. NUMBER OF PAGES
emissions, nitrogen oxide, turbocharged diesel	16. PRICE CODE

17. SECURITY CLASSIFICATION OF REPORT	18. SECURITY CLASSIFICATION OF THIS PAGE	19. SECURITY CLASSIFICATION OF ABSTRACT	20. LIMITATION OF ABSTRACT
UNCLASSIFIED	UNCLASSIFIED	UNCLASSIFIED	UL

SAE TECHNICAL
PAPER SERIES

942046

Cylinder-Averaged Histories of Nitrogen Oxide in a D.I. Diesel with Simulated Turbocharging

Ronald J. Donahue, Gary L. Borman, and Glenn R. Bower
University of Wisconsin-Madison

SAE The Engineering Society For Advancing Mobility Land Sea Air and Space®
INTERNATIONAL

Fuels & Lubricants
Meeting & Exposition
Baltimore, Maryland
October 17-20, 1994

400 Commonwealth Drive, Warrendale, PA 15096-0001 U.S.A. Tel: (412)776-4841 Fax:(412)776-5760

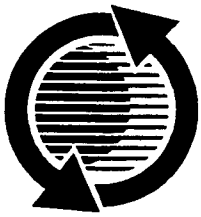

ISSN 0148-7191

Printed in USA

90-1203C/PG

942046

Cylinder-Averaged Histories of Nitrogen Oxide in a D.I. Diesel with Simulated Turbocharging

Ronald J. Donahue, Gary L. Borman, and Glenn R. Bower
University of Wisconsin-Madison

ABSTRACT

An experimental study was conducted using the dumping technique (total cylinder sampling) to produce cylinder mass-averaged nitric oxide histories.

Data were taken using a four stroke diesel research engine employing a quiescent chamber, high pressure direct injection fuel system, and simulated turbocharging. Two fuels were used to determine fuel cetane number effects. Two loads were run, one at an equivalence ratio of 0.5 and the other at a ratio of 0.3. The engine speed was held constant at 1500 rpm. Under the turbocharged and retarded timing conditions of this study, nitric oxide was produced up to the point of about 85% mass burned.

Two different models were used to simulate the engine run conditions: the phenomenological Hiroyasu spray-combustion model, and the three dimensional, U.W.-ERC modified KIVA-II computational fluid dynamic code. Both of the models predicted the correct nitric oxide trend. Although the modified KIVA-II combustion model using Zeldovich kinetics correctly predicted the shapes of the nitric oxide histories, it did not predict the exhaust concentrations without arbitrary adjustment based on experimental values.

INTRODUCTION

Obtaining lower nitrogen oxides (NO_x) emissions from diesel engines without compromise of particulate emissions standards, fuel economy or durability is a continuing problem for combustion engineers. If cost effective lean burn catalysts (1*) or fuel additives (2) can be found, the need for combustion modifications may be reduced. Until this happens, the major methods of reduction remain: retarded injection timing; lower air inlet temperature; boosted inlet pressure; exhaust gas recirculation (EGR); and fuel reformulation (3). Application of these methods may, of course, produce some conflicting effects. For example, retarded injection timing and higher fuel cetane number reduce the amount of ignition delay and thus the premixed burn fraction, but reduced air inlet temperature and EGR, while lowering flame temperature, tend to increase the ignition delay. Nevertheless, the overall trend has been to reduce the premixed burning spikes so that almost all the combustion is mixing controlled. Thus, the modern heavy duty direct injection diesel exhibits a significantly different combustion process from the naturally aspirated (n.a.) lower injection pressure engines of the past. These changes raise an important question. How well does the understanding of the NO_x formation process in older engines (4) translate to modern engines?

In the late 1970's the experimental technique of dumping (total cylinder sampling) was applied to an n.a. open chamber diesel to produce histories that were then compared to some of the existing phenomenological models (7,8,9.) Both the Cummins (8) and the U. Hiroshima (9) models reproduced the experimentally observed trends reasonably well. The concept which emerged from these and other studies was that NO could be calculated by application of the extended Zeldovich mechanism (10) to the products of combustion. Most of the NO was found to be produced in the products formed by the premixed burning portion of the combustion history.

Using this concept, a first approximation to the total NO_x produced could be obtained by calculating the amount of equilibrium NO in the products existing at the time of peak pressure. Approximation of the mass of products can be obtained from a single zone heat release analysis (11). Furthermore, because the rapid premixed combustion dominated, the temperature could be approximated as uniform at the adiabatic flame temperature for a stoichiometric mixture (12).

When applied to modern engines, the accuracy of such simple algorithms is questionable. Fortunately, much more complete computational fluid dynamics (CFD) (13) and more sophisticated phenomenological

* Numbers in parenthesis refer to references as listed at end of paper.

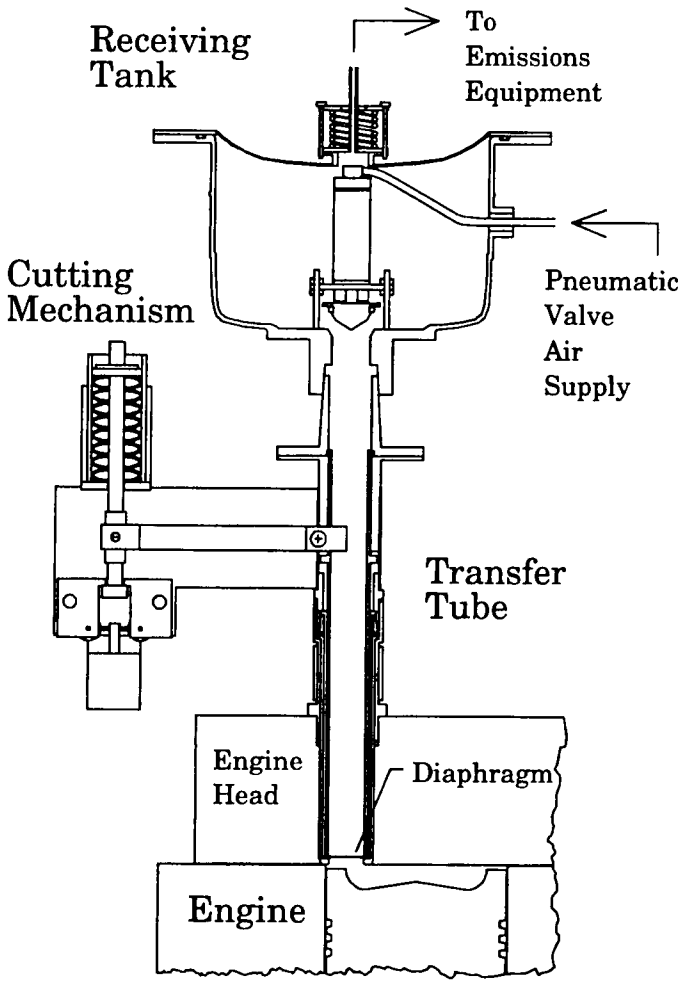

Figure 1. Schematic diagram of the dumping mechanism.

models (14) are now available. What was lacking, however, were dumping data similar to those of Refs. 4 and 5 but obtained for a modern turbocharged engine. This study was undertaken to provide a modest amount of such data which could then serve as a starting point for comparison with CFD models (15,16) and phenomenological models (14).

EXPERIMENTAL DATA

The concept of the experimental method used in this study is to rapidly quench the NO reactions in the engine cylinder at a given crankangle by causing the cylinder contents to rapidly flow from the cylinder into a large evacuated receiving tank. Analysis of the receiving tank contents gives an approximation to the mass averaged concentration of NO in the cylinder at the given crankangle. Repetition of the experiment at different crankangles then gives a history of cylinder average NO for a given operating condition.

The basic idea of the experiment was developed by Roblee (17) and applied to rapid compression machines by Roblee and others (18,19,20). It was first applied to a diesel by Voiculescu (21) in his Ph.D. thesis at U.W.-Madison. Subsequent work on the apparatus by Chan (22), Thien (23) and Van Gerpen (24) produced various mechanical improvements. The existing apparatus, as redesigned by Van Gerpen, was used in this experiment with some additional modifications, here noted. A more detailed history is found in Donahue's thesis (25).

Figure 1 shows a diagram of the mechanical system used to sample the cylinder gas. Figure 2 shows a more detailed diagram of the engine cylinder end of the mechanism. In this design a stack of 26 pairs of Belleville Washers provides a force of about 2,670 N which, with the 8:1 lever arm, causes a force of 21,360 N to be applied to the cutter. This causes the 35 mm diameter Paint-Loc steel diaphragm of 0.61 mm thickness to be sheared. The cylinder pressure then causes the diaphragm to move upward around the crossing body, like the wings of a butterfly. The inner diameter of the transfer tube is 24.5 mm. The distance from the diaphragm plane to the pneumatic valve seat is 38.6 cm. The pneumatic valve closing apparatus is a modification made for this study to provide a rapid means of isolating the cylinder from the receiving tank contents at the end of the dumping process. The previous design used a ball value mounted in the transfer tube. In addition, the engine valves are deactivated at the time of dumping in order to keep the cylinder pressure low and thus prevent the pneumatic valve from being pushed open again by the cylinder gas pressure.

The pneumatic valve was closed at about 30 crank degrees after the start of diaphragm cutting. The valve has a cone shape to minimize possible effects of reflected shocks traveling down the transfer tube. At the time of dumping, a solenoid was used to pull the rack on the fuel injector in order to stop the fuel injection as quickly as possible.

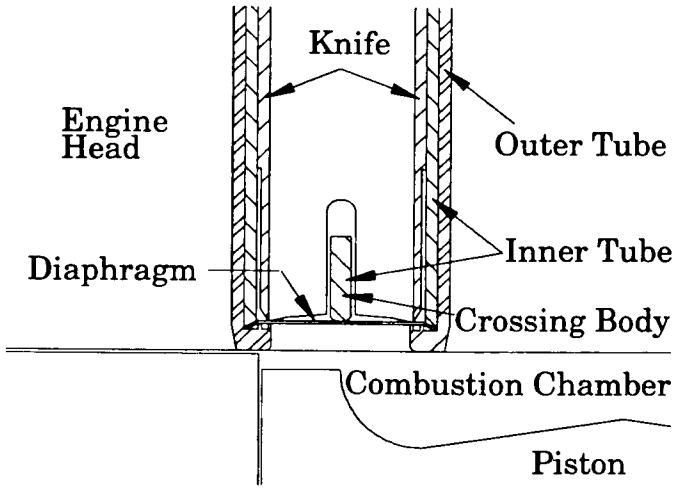

Figure 2. Schematic diagram of the diaphragm and lower end of the cutting mechanism.

All the events described above were controlled by timing circuits with delays set so as to off-set the various mechanical delays. Using these trigger circuits, the dumping crankangle at 1500 rpm could be predetermined to within ± 5°.

After dumping, the receiving tank, with a volume of 6.2 displacement volumes, was filled to 274 KPa (25 psig) with a reference mixture of 660 ppm CH_4 in N_2 gas. The collected mixture composition was then determined by use of a Fourier Transform Infra Red (FTIR) spectrometer supplied by Nicolet Instruments. The measured concentration of methane was used to correct the concentrations of the collected gas for dilution. Use of the known gas mixtures in the dump tank allowed evaluation of the dilution technique, showing the measurement of the undiluted mixture concentration to be within ± 5 percent.

THE ENGINE

The engine used in this study is a modified version of a single cylinder TACOM/LABECO research engine (26). The engine head, piston bowl and injection system are different from the original design. In particular, the engine head contains a 38 mm diameter instrumentation port that allows access to the combustion chamber. For this study, the engine head also contained the dumping port shown in Figs. 1 and 3. Table 1 gives the specifications for the modified engine. Figure 4 gives the injection pressure and flow rate histories for two rack settings.

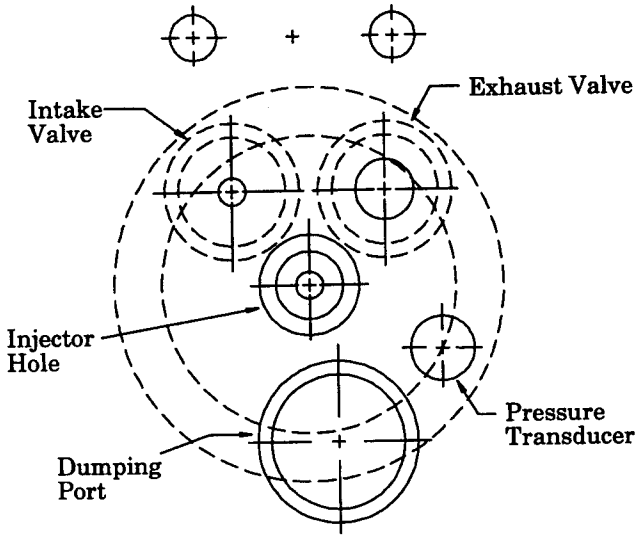

Figure 3. Simplified plan view of the engine head as viewed from the top.

TABLE 1
Modified TACOM/LABECO Engine Specifications

4-Stroke Cycle	
Bore	114.3 mm (4.5 in.)
Stroke	114.3 mm (4.5 in.)
Connecting Rod Length	228.6 mm (9.0 in.)
Displacement	1172.8 cc (71.57 in^3)
Compression Ratio	16:1
Valve Timing	
Intake	Opens at TDC
	Closes at 40° abdc
Exhaust	Opens at 40° bbdc
	Closes at TDC
Mexican Hat Type Combustion Chamber	
Bowl Diameter	88.9 mm (3.5 in.)
Maximum Depth	12.7 mm (0.5 in.)
Injection System	
Robert Bosch Model P-6000 Pump	
American Bosch Model AKN-90M-6425A Nozzle Holder	
8 x 0.18 x 165° cone-angle nozzle	
Peak Injection Pressure 65 MPa (9500 psi)	

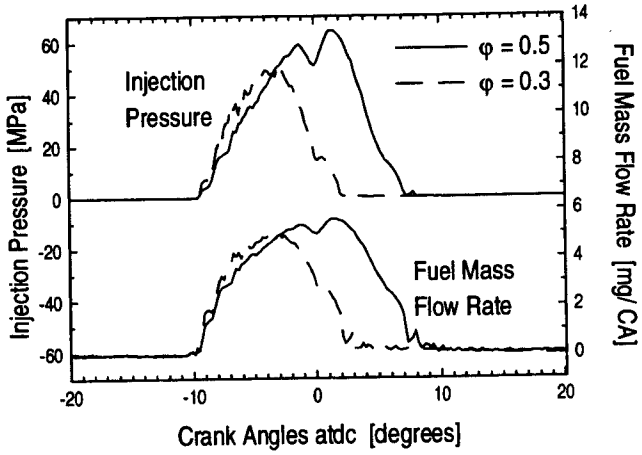

Figure 4. Injection pressure and fuel mass flow rate histories corresponding to equivalence ratios of 0.3 and 0.5 for D-2 fuel.

ENGINE INSTRUMENTATION

Figure 5 shows a schematic of the engine setup and related equipment. The dynamometer and its controller allowed the engine speed to be held to within two rpm of a set point. The fuel flow was measured with a Flowtron system that gives flow rates to within one percent. The AVL variable timing device and Hall-effect needle lift indicator allowed injection timing to be set to within 0.2 crank degrees over a 12 degree window. The engine coolant temperature was controlled to ± 2°C

under steady-state operation. The intake air temperature was held to within 2°C and the intake surge tank pressure to within 1.379 KPa (0.2 psi). The intake and exhaust surge tanks are each about 100 displacement volumes. The air mass flow was measured using calibrated critical flow nozzles. The cylinder pressure was measured using an AVL 12 QP 505 clk water cooled transducer flush mounted and used without RTV coating. The dump tank pressure was measured with a Kistler model 601A transducer. The crankangle was determined at 0.2 degree intervals with an optical shaft encoder. Cylinder pressure, receiving tank pressure, needle lift and the dump trigger signal were recorded using a four channel data acquisition system (27).

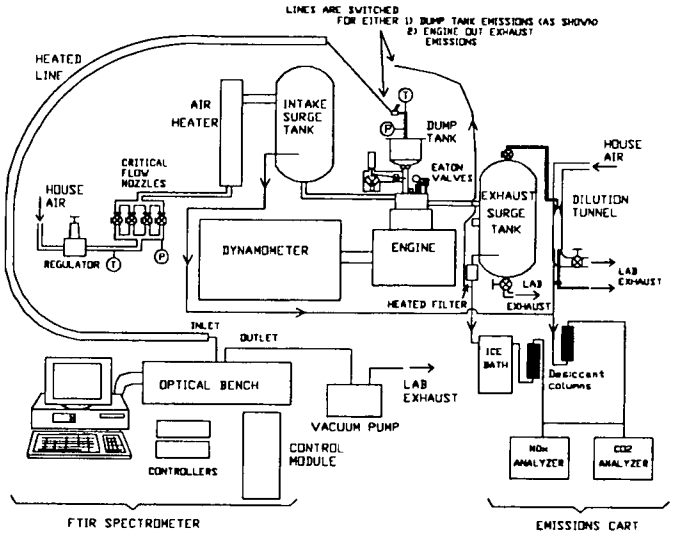

Figure 5. Schematic of the engine setup and related equipment.

EXPERIMENTAL CONDITIONS

Dumping history data were taken for a fixed speed of 1500 rpm with an intake tank pressure of 179 KPa (26 psia) and exhaust tank pressure of 193 (28 psia). The start of injection (SOI) was held fixed at 9 crank degrees before top dead center. This SOI value was based on the data of Figure 6 which shows a particulate -- NO trade-off curve obtained by Shamis (29) at the conditions of dumping run number 1. The four steady-state conditions used for the dumping study are shown in Table 2 which also shows performance and emissions data for these conditions. The two fuels used were a low sulfur fuel supplied by Amoco (30) and a low sulfur, high natural cetane fuel supplied by Chevron Research (31). Table 3 shows some of the properties of these fuels. Note that the fuel with natural high cetane number has a lower 50% temperature on the distillation curve and almost zero aromatics content.

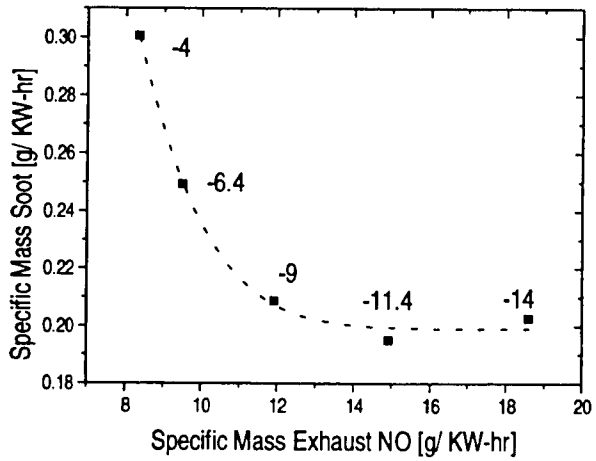

Figure 6. Exhaust NO and soot mass for full load at various injection timings.

As previously mentioned, an FTIR spectrometer was used to determine the gas species concentrations in the diluted contents of the receiving tank and the undiluted exhaust gas. These measurements were checked against those made with standard chemiluminescent (CLA) and nondispersive infrared (NDIR) analyzers.

In this study, no attempt was made to determine the particulate mass within the receiving tank after a dump, as has been done in a series of experiments at the University of Minnesota (28). However, exhaust particulate mass was measured for the same engine operating conditions used in the dumping experiments by use of a minidilution tunnel (25). Reproducibility of these cycle averaged data was excellent, but the experiment could not measure cyclic variability of the particulate.

TABLE 2
Engine Operating Conditions

Run No.	1	2	3	4
Fuel Cetane No.	48	62.5	62.5	48
Equiv. ratio, ϕ	0.5	0.5	0.3	0.3
T_{in} (°K)	333	333	333	333
Exhaust NO (g/Kg fuel)	46.97	43.09	38.75	50.08
Exhaust Particulate (g/Kg fuel)	0.7935	0.5069	----	----
IMEP (MPa)	1.031	1.034	0.622	0.636
Isfc (Kg/MW-s)	0.055	.0542	.0535	.0520
Peak Press (MPa) (average of 120 cycles)	9.749	9.632	8.687	8.997

TABLE 3 Test Fuel Properties		
Property	D-2 Fuel	Low Aromatic Fuel
Cetane No	48	62.5
Density (kg/m^3)	846	800
Viscosity @ 40 °C (cs)	2.81	2.38
Elemental Analysis		
Carbon, wt. %	86.36	85.95
Hydrogen, wt. %	13.30	13.68
Carbon/Hydrogen Ratio	6.493	6.283
Sulfur, wt. %	0.031	0.005
L.H.V. (KJ/Kg)	43,073	43,745
Aromatics, Volume %	28	1.1
Distillation: K		
IBP	479	---------
10	500	483
50	536	521
90	580	590
EP	601	607

CYCLIC VARIATION

Because the data for a single NO history were gathered from different cycles, it is expected that cyclic variability of the combustion will produce scatter. The only direct method of judging the variability of global NO in the cylinder is the scatter in the dumping data itself. Unfortunately, such scatter represents many sources of error. Thus it is difficult to determine what fraction of observed scatter is due to actual cyclic variations of NO. For example, small errors in crank angle determination can cause large apparent scatter during the most interesting portion of the history when the NO value is rising rapidly. Indirect evidence of combustion stability was obtained from the needle lift and pressure data. Variations in the start of injection (SOI) were less than 0.4 crank degrees and standard deviation of the cylinder pressure was less than 1%. Variations in ignition delay and premixed burning rate would provide even more direct evidence of stability, but these are difficult to obtain because of the small size of the pressure changes that cause them. Despite this difficulty, analysis of the ensemble average pressure is nevertheless possible and gives information about the combustion histories that may be helpful when interpreting the dumping data.

ANALYSIS OF ENSEMBLE AVERAGED PRESSURE

Ignition delay and heat release were obtained by application of a single zone heat release model which uses the experimental pressure data to predict an

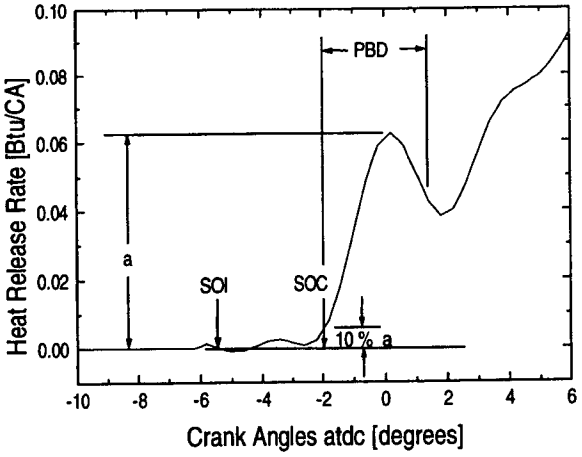

Figure 7. Heat release history showing definition of start-of-combustion (SOC) and premixed burning duration (PBD) relative to start-of-injection (SOI).

apparent burning rate (32). The ignition delay was defined by the needle lift data and the crankangle of the start of combustion, defined by the crankangle at which 10% of the premixed burning spike was reached. This is illustrated in Figure 7.. Note that the location defining the end of premixed burning is the inflection point of the negative slope.

Table 4 shows a summary of heat release parameters for the four conditions of Table 2. Note that the definition of the start-of-combustion (SOC) used here gave consistent data when plotting ignition delay versus start of injection (SOI) and ignition delay as a function of the reciprocal of mass-average-temperature during the delay period. Other definitions, such as using the zero crossing point of the heat release, did not give such consistency.

Comparisons of premixed burn fraction (PBF) and exhaust NO show the expected effects of cetane number at the high load (Runs 1 and 2). However, the difference in ignition delay is very small so that the

TABLE 4 Summary of Heat Release Data (Operating Conditions of Table 2)				
Run No.	1	2	3	4
Ignition Delay, CA° (soi @ 9° btdc)	3.88	3.20	3.32	3.63
Premixed Burn Duration, CA°	3.02	2.60	2.88	1.77
Premixed Burn Mass, mg	3.38	1.84	2.62	2.14
Crank Angle of Peak Press., CA° atdc	10.0	10.2	7.6	7.0
Mass Burned @ Peak Pressure, mg	30.36	20.55	17.36	18.72

expected increase in PBF due to a longer time for vaporization and mixing before ignition is not plausible. An argument based on volatility is contradicted by the fact that higher cetane fuel, as determined by the distillation data, is more volatile.

Runs 3 and 4 were carried out at decreased load, but with the same inlet pressure and temperature so as not to confound the results by an assumed turbocharger performance factor. Thus, the ignition delay is about the same as at the higher load. The mass of fuel burned during the premixed burning decreased with load for the lower cetane fuel, but unexpectedly increased slightly for the high cetane fuel. Apparently, the full load high cetane fuel premixed burn mass is smaller than anticipated. Figure 8 shows a comparison of the heat release histories for the two fuels at the higher load and Figure 9 shows the comparison at the lower load. A careful comparison of the injection rate diagrams (Figure 4) for the two loads shows that an additional 1.6 mg. of fuel was injected during the premixed period at the lower load. It appears that the more volatile, high cetane fuel could vaporize and burn some of this additional fuel, while the D-2 fuel premixed burning was limited by mixing rates and thus did not have a significant increase in the premixed burning due to the extra fuel injected.

ANALYSIS OF THE QUENCHING PROCESS

For the concept of the dumping technique to be valid, the temperature of the products produced at the time of dumping must decrease rapidly enough to prevent significant formation of NO during the dumping event. It is also important that any new products formed during the dump not produce significant NO.

The simplest analysis is to assume that no new products are formed during the dump and that the existing products remaining in the cylinder are expanded adiabatically. The expansion pressure for such products is assumed to be the measured cylinder pressure. Such

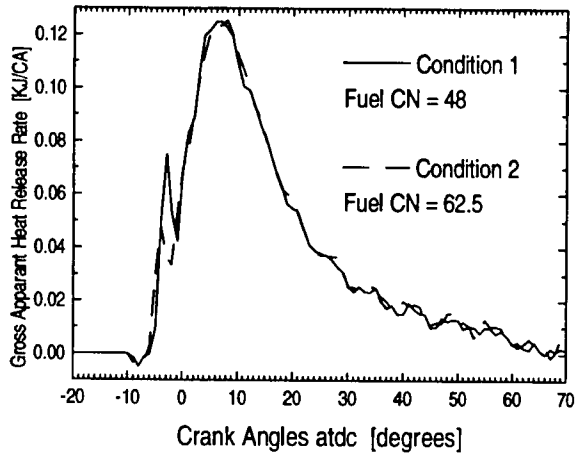

Figure 8. Comparison of heat release histories for two fuels at the same engine condition; Runs 1 and 2 of Table 4.

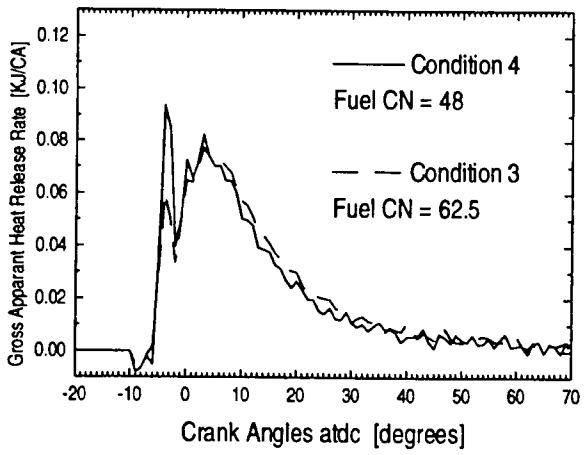

Figure 9. Comparison of heat release histories for two fuels at the same engine condition; Runs 3 and 4 of Table 4.

an analysis shows that the NO will be frozen for typical dumping expansion times as experienced by Voiculescu (5,21). This, however, is a very optimistic analysis. A more pessimistic estimate is to assume that NO is produced throughout the dumping event at the same rate as predicted by the dumping experimental history. Using this analysis, each experimental data point would be retarded by the crankangle interval of the dump for that point to produce a corrected point. Thus, for example, if each dump had a three degree interval history, the data history would be retarded by three degrees to produce the corrected history.

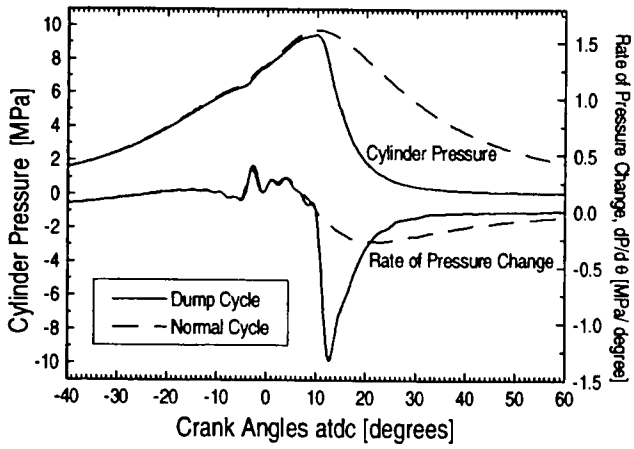

Figure 10. Normal ensemble-averaged and dumping cycle pressure data history for conditions of Run 1 of Table 4. Upper (a) shows pressure and lower (b) shows pressure derivative. Dumping was initiated at 10 CA° atdc for the data shown.

The effect of the transfer tube is not included in either of the above estimations. Recent calculations and experimental investigations by Kato, Bower and Foster (33) indicate that NO production in the transfer tube is quenched so that it does not cause a significant error in measured NO. Their experiments further indicate that reactions in the transfer tube do change the amount of CO and CO_2 collected. Therefore, data for CO and CO_2 collected in the present study are not reported here.

Figure 10a shows the measured cylinder pressure history for a normal and a dump cycle at the conditions of run 1. The dump for this cycle was at 10 CA° atdc. This is shown more clearly in Figure 10b, which gives dp/dθ for the histories in Figure 10a. The quench period and dp/dθ values depend on the pressure at the time of dump. In the case shown, the pressure was nearly maximum at the time of dump and thus, the duration was short (2.5 CA° or 0.28 ms) and the value of dp/dθ was large (-1.30 MPa/CA°). Values of dp/dθ ranged from -1.3 to -0.7 MPa/CA° and dumping durations from 2 to 4 CA°. Dumps taken at the same pressure level show a slight effect of heat release when the dump takes place during a high rate of heat release. High rates of heat release slightly reduce the rate of pressure change, indicating some continuing heat releases during the dumping event. In summary, the rates of temperature reduction are similar to or greater than in prior works (5,20) and appear to be sufficient to quench the NO reactions.

DUMPING RESULTS

Figures 11 and 12 show the data from dumping for Runs 1 and 2 of Tables 2 and 4. In each case, the data were fitted with a formula selected to provide the observed "S" shape of the data. In each case, the curve was forced to pass through the measured exhaust value. The equation used for fitting is the so called logistic growth curve given by

$$NO = \frac{NO_{res} * NO_{exh}}{NO_{res} + (NO_{exh} - NO_{res}) * e^{-r(CA-CA_{start})}} \quad (1)$$

where NO_{res} = residual NO concentration
NO_{exh} = exhaust NO concentration
$CA\text{-}CA_{start}$ = crankangle with zero set at start of NO rise
r = arbitrary fitting parameter

The value of r was selected by least squares analysis using predetermined values of NO_{res}, NO_{exh}, CA_{start}, and neglecting outliers only in the region beyond the knee in the curve. Because there was no way to measure cyclic variations of the exhaust NO, it cannot be determined to what extent the scatter in the data beyond the upper knee of the curve is due to such variations. During the generation of a dumping history exhaust NO was noted to vary by as much as 200 ppm. This represents a minimum expected scatter due to cyclic variability.

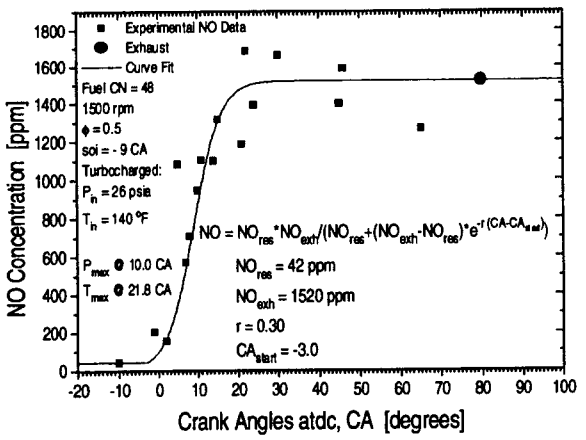

Figure 11. Dumping NO data points and curve fit for conditions of Run 1 of Table 4.

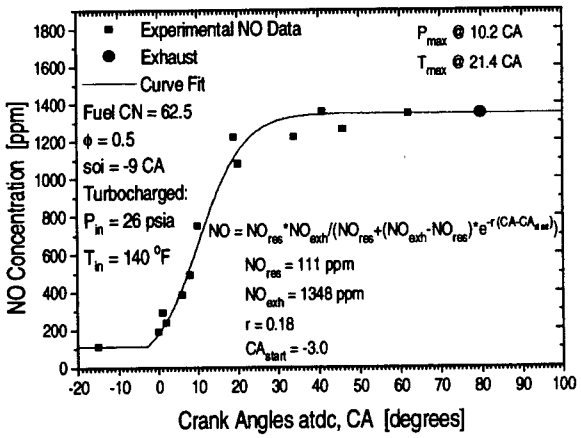

Figure 12. Dumping NO data points and curve fit for conditions of Run 2 of Table 4.

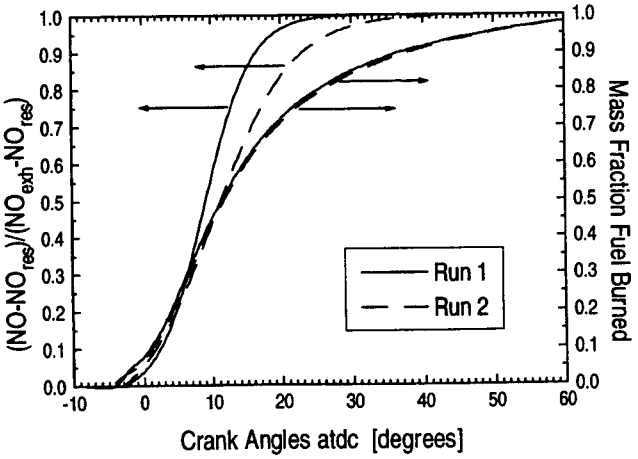

Figure 13. Curve fits from Figures 11 and 12 and corresponding mass burned fractions for conditions of Runs 1 and 2 of Table 4.

Comparison of Figs 11 and 12 shows less variability for the low aromatic fuel. In part this difference is believed to be due to improved reliability of the FTIR during the runs of Fig 12. Quantification of the many sources of scatter in both magnitude and timing was found to be beyond our ability.

Note that for the -9 SOI timing, very little NO has been formed by TDC, but that by peak pressure about 60% of the NO has been produced. Figure 13 shows the curve fits of Figure 11 and 12 in the normalized form and the mass burned fraction for each. The 62.5 cetane fuel has both a lower exhaust value and a lower slope during the rising portion of the history than the 48 cetane fuel. Note that the effect of the very low aromatic content of the 62.5 cetane fuel is confounded by the cetane number effect. For the 48 cetane fuel, the fraction of NO formed and the fraction of mass burned are equal at the 45% point, which is also close to the maximum slope of the NO history. This point is slightly beyond the peak in the diffusion burning portion of the heat release. The formation of NO is thus much slower and, apparently, less dominated by the premixed burning than in prior data for naturally aspirated engines run at the more advanced injection timing corresponding to MBT. For the Run 1 data the premixed burn fraction is only 0.05. If this premixed product is formed at an equivalence ratio of 0.9 and then compressed to peak pressure it will have a temperature of about 2900 K and produce an equilibrium NO concentration of 700 ppm in the cylinder volume. This is about 46% of the NO in the exhaust and about 70% of the NO produced up to the time of peak pressure. It should be emphasized that the premixed products may produce less than the maximum due to mixing and heat loss.

The data for two fuels at an equivalence ratio of 0.3 (runs 3 and 4) are shown in Figure 14, along with the curve fit for each. Note the large amount of scatter which makes the distinction between the runs depend on the exhaust values. A better fit of the data points, using some other fitting equation, would result in an asymptote

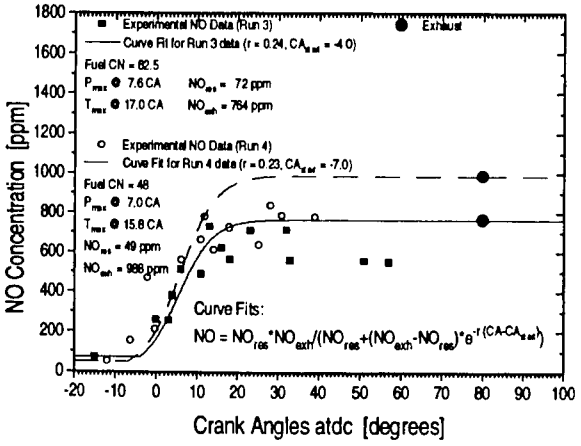

Figure 14. Dumping NO data points and corresponding curve fits for conditions of Runs 3 and 4 of Table 4.

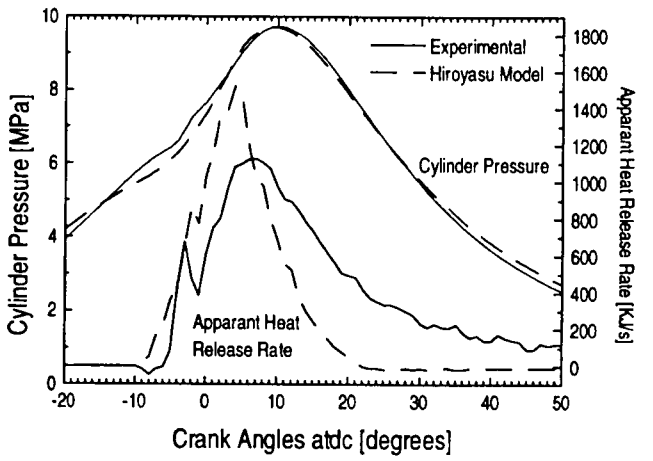

Figure 15. Comparison of pressure and heat release data for Run 1 with computed results using model of Ref. 14.

falling well below the measured exhaust concentration. The heat release rates for these two runs are very similar except for the much larger, premixed burn spike of the 48 CN fuel. The 30% higher exhaust NO for the lower cetane fuel would appear to be caused by the larger premixed burn fraction. However, this premixed burn products mass is compressed much less than for the higher loads of runs 1 and 2 and thus should produce less NO.

MODELING RESULTS

Simple models for the production of NO in engines can be based with some success, on equilibrium considerations (12). However, such models typically give an estimate of potential NO formation based on assuming the fuel-air ratios of the product and using simplified mixing rules. The models compared to

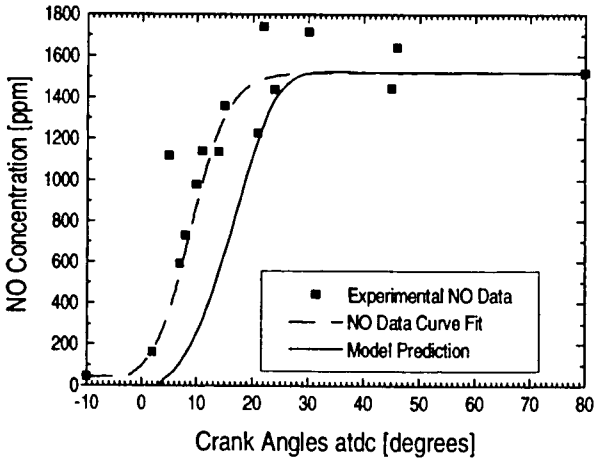

Figure 16. Comparison of dumping NO data and results of model of Ref. 14 for conditions of Run 1.

dumping experimental data in Ref. 5 used phenomenological models to provide the required fuel-air ratios and typically lumped all products into a single system. Zeldovich kinetics were then used to calculate the NO formed in the products system. One of these models, that of Hiroyasu and coworkers (9) at the University of Hiroshima, has been greatly improved in detail (14) while still providing a computation capable of being run on a P.C. workstation. Some alternatives to such a phenomenological model are the computational fluid dynamics models such as KIVA (13,15) which require super computers for practical run times. Both the KIVA and University of Hiroshima models (14,15) were used to compare to the present data obtained with the lower cetane D-2 fuel. It was not felt that either model could respond to fuel property changes without considerable ad hoc adjustment and thus, computations were not made for the high cetane fuel.

The University of Hiroshima model predicted the general shape of the cylinder pressure, but did not predict the heat release shape. Figure 15 shows the comparison of the heat release and pressure and Figure 16 shows the comparison of the NO profiles for Run 1. The excellent agreement with the NO data seems fortuitous considering the difference in heat release shape. However, these results may not show an optimum comparison, because the authors were not well enough acquainted with the parameter selection procedures for the model.

Figure 17 a and b shows the pressure and heat release comparisons between KIVA results and the experimental data runs for 1 and 4, respectively. Although KIVA predicted too much mass burning before TDC, the NO values required a large adjustment upward. Results from tests on a different engine (16) indicated that an arbitrary factor of 2.5 was needed to match exhaust NO values. This same factor was applied here and gave the excellent results shown in Figure 18 a and b. Figure 19 shows temperature and NO contours for Run 1 at four different crankangles. Note that the high temperature is close to the cylinder axis rather than near the edge of the bowl, indicating less mixing than might be anticipated. Figure 20 shows some predicted values of characteristic temperatures. The minimum and maximum cell temperatures at each crankangle were found to be quite different from the mass average temperatures, even at 60 CA° atdc. The history marked T_{NO} was defined by

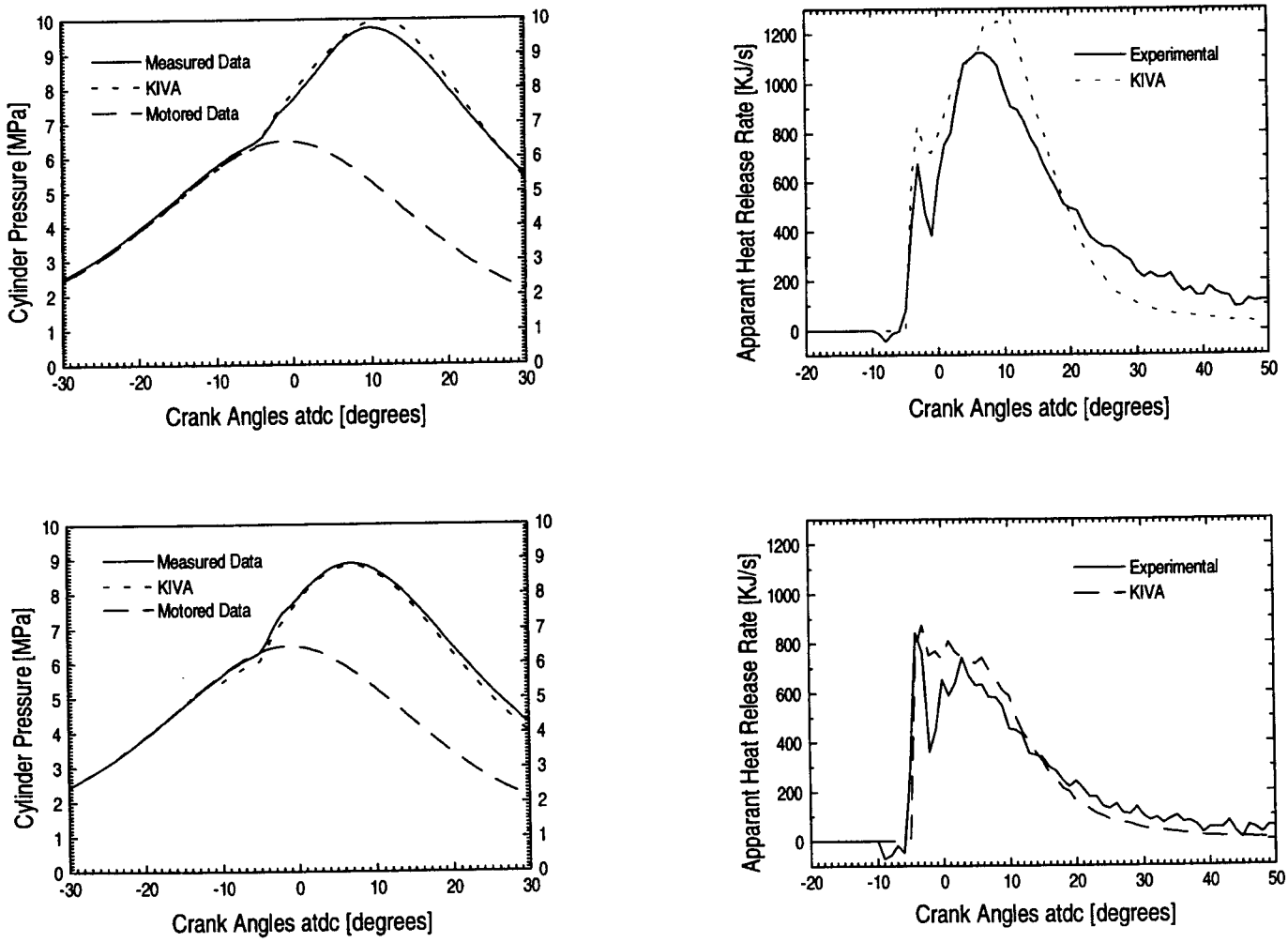

Figure 17. Comparison of pressure and heat release data for (a) Run 1 (upper) and (b) Run 4 (lower) with computations using KIVA code (15).

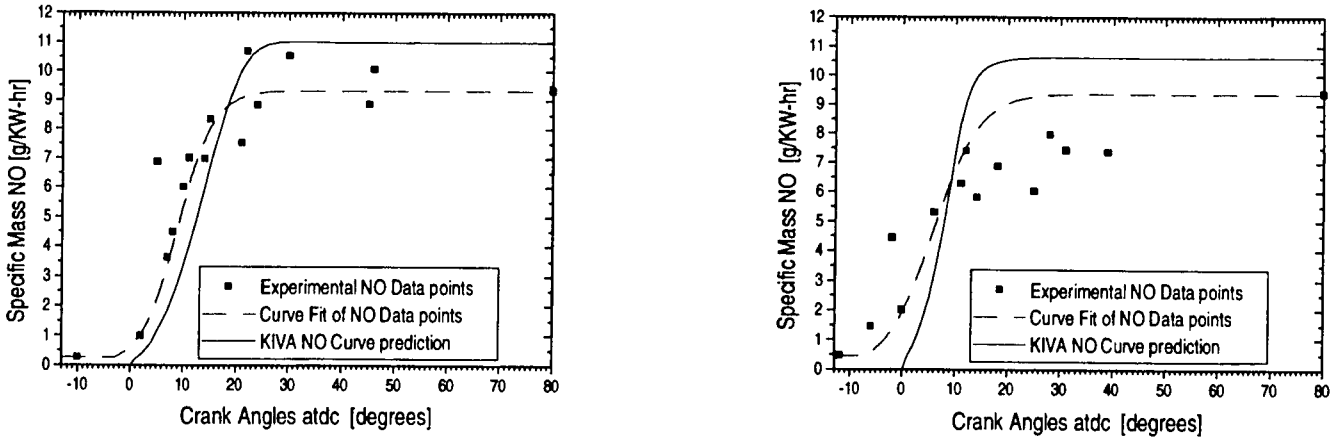

Figure 18. Comparisons of dumping NO data and results of KIVA code (15) for (a) Run 1 (left) and (b) Run 4 (right).

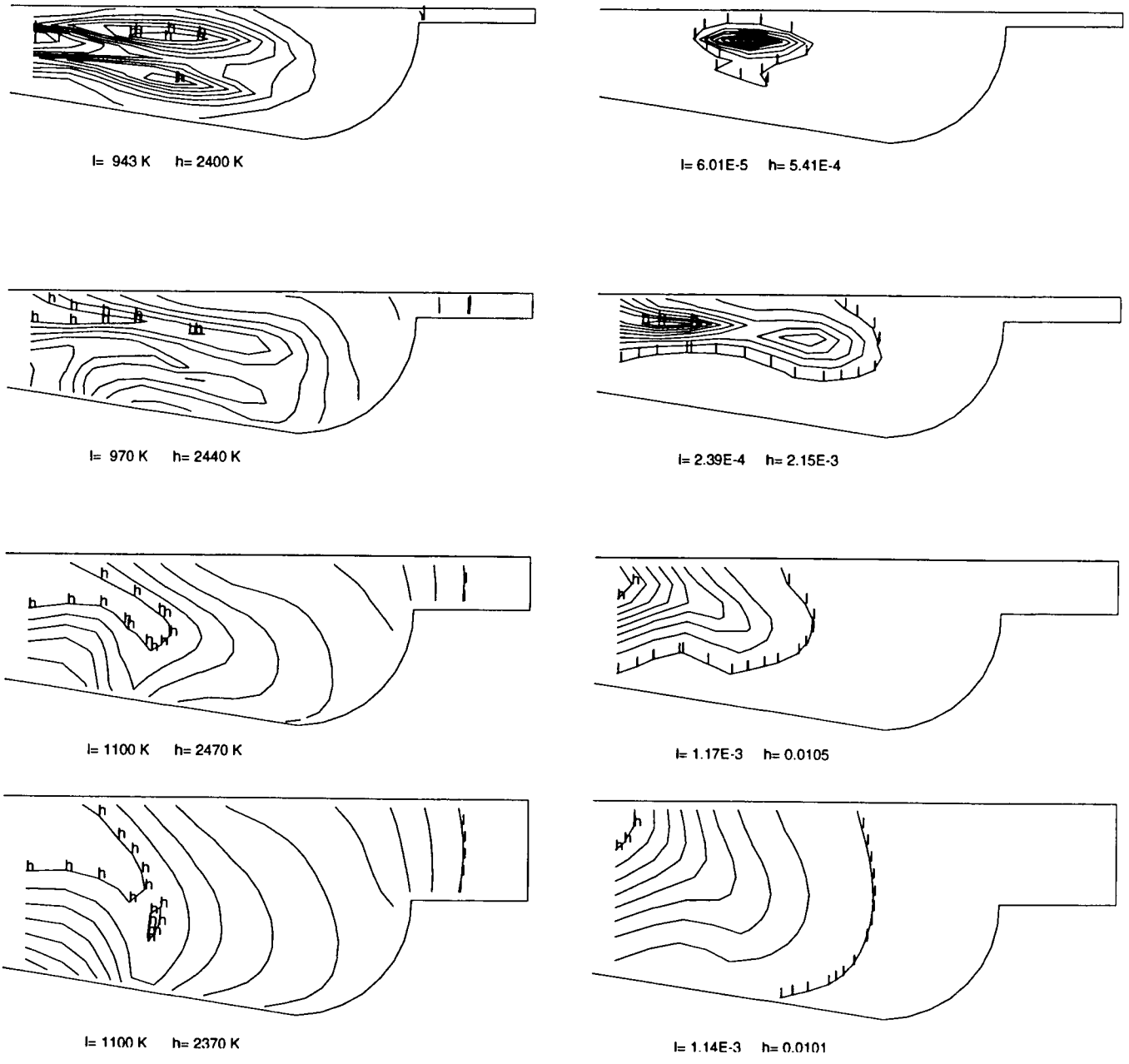

Figure 19. Contour plots from KIVA calculations for Run 1 conditions showing temperature (on left) and NO mass-fraction (on right) concentrations for TDC, 10, 20, and 30 degrees atdc. Plane shown is through spray axis.

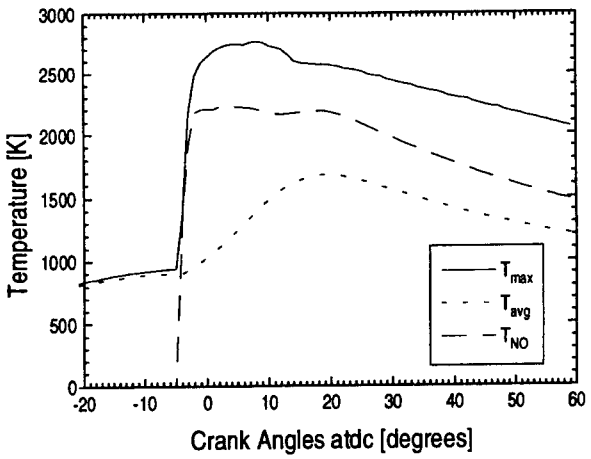

Figure 20. Plot showing various calculated temperature histories corresponding to Figure 19.

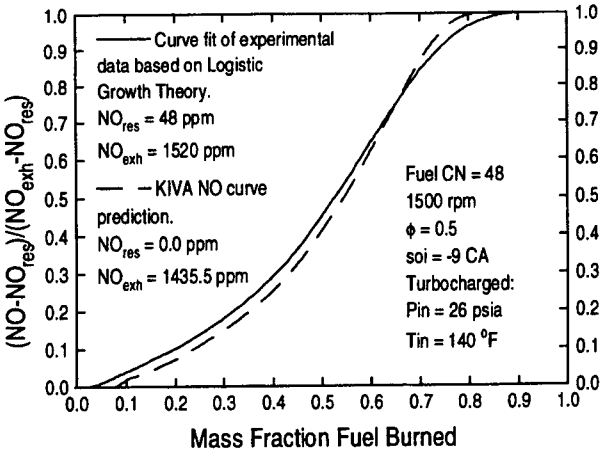

Figure 21. Normalized NO versus mass burned fraction obtained from fit of dumping data and KIVA calculation for Run 1.

$$T_{NO} = \sum_{i=1}^{N} (M_{NO})_i \, T_i \Big/ \sum_{i=1}^{N} (M_{NO})_i \qquad (2)$$

where $(M_{NO})_i$ = mass of NO in cell i
T_i = temperature of cell i

The T_{NO} value is just above 2200 K for a long period indicating the reason that the NO forms slowly. Freezing of the NO reactions below 2100K is expected from the kinetics, and thus the nearly constant value of NO beyond 23 CA° atdc, as shown in Figure 18, is explained by Figure 20.

Flame temperatures measured (34) in turbocharged diesels at full load are typically in the range of 2700-2800 K. For the conditions of Run 1 products formed during the period from SOC to peak pressure will be in this range if they have an equivalence ratio, ϕ, of about 1.3 to 1.4. To obtain the low products temperature of 2200 K predicted by KIVA requires an equivalence ratio of about 2.3. The equilibrium NO at 2800 K and ϕ = 1.4 is 470 ppm. At 2200 K and ϕ = 2.3 the NO is 1 ppm. This indicates that KIVA could give the correct NO levels by only small changes in the mass-temperature distribution that goes into Eq. 2.

The current KIVA calculation using the arbitrary correction factor did give an excellent agreement with the shape of the NO history found from dumping as illustrated by Fig. 21. This leaves the puzzle of how the calculated shape might change if new KIVA models gave better agreement with heat release and NO levels.

SUMMARY

The NO history data for a turbocharged engine with retarded timing show that NO is produced throughout the burning period in such engines. This indicates that models for predictions of NO in these engines require more sophisticated mixing and combustion sub-grid models than do older engine designs in which NO production is dominated by the premixed combustion phase.

Although current models correctly predict trends of NO versus crankangle, they fail to simultaneously predict combustion rates and NO levels. Combining dumping with 2-D imaging of temperature and fuel and air ratios could prove helpful in sorting out the needed improvements for the models. Measurements of cycle-by-cycle variations of exhaust NO, coupled with dumping data, could also be helpful in determining the sources of scatter observed in the dumping data. It is hoped this paper encourages such research approaches.

ACKNOWLEDGMENTS

This research was made possible by funding from the Dept. of Energy, Office of Transportation Technologies, under subcontract number 19X-SK396C with Martin Marietta Systems, Inc., and funding by the Army Research Office through Grant DAAL03-92-G-0122. Technical support and gifts-in-kind were provided by Amoco, Chevron Research, and Nicolet Instrument Co. Among the many colleagues at the ERC, the authors thank especially Professor David Foster, Dmitry Shamis, and Dale Tree for their help with the experimental work and S.C. Kong, G. Hampson and M. Patterson for their help with the computer simulations.

REFERENCES

1. Tsuchida, H., Tabata, M., Miyamoto, K., Yoshinari, T., Yamasaki, H., Hamada, H., Kintaichi, Y., Sasaki, M., Ito, T., Nakatsuki, T., and Yoshimoto M., "Catalytic Performance of Alumina for NO_X Control on Diesel Exhaust," SAE Paper 940242 (1994).

2. Tree, D., Bower, G., Donahue, R., Shamis, D., and Foster, D., "Emission Tests of Diesel Fuel with NOx Reduction Additives," SAE Paper 932736 (1993).

3. Borman, G.L. and Brown, W.L., "Pathways to Emissions Reduction in Deisel Engines," Second International Engine Combustion Workshop, C.N.R., Capri, Italy (1992).

4. Yu, R.C., and Shahed, S.M., "Effects of Injection Timing and Exhaust Gas Recirculation on Emissions from D.I. Diesel Engine, SAE Paper 811234 (1981).

5. Voiculescu, I.A., and Borman, G.L., "An Experimental Study of Diesel Engine Cylinder-Averaged NO_X Histories," SAE Paper 780228 (1978).

6. Chan, T.T., and Borman, G.L., "An Experimental Study of Swirl and EGR Effects on Diesel Combustion by Use of the Dumping Method," SAE Paper 820359 (1989).

7. Kau, C.J., Tyson, T.J., Heap, M.P., "The Prediction of Pollution Formation in Diesel Engines," Final Report Phase II and III, APRAC Project CAPE 20-17, Ultrasystems Inc., (1976).

8. Chiu, W.S., Shahed, S. M., and Lyn, W.T., "A Transient Spray Mixing Model for Diesel Combustion," SAE Paper 760128 (1976).

9. Hiroyasu, H., and Kadota, T., "Models for Combustion and Formation of Nitric Oxide and Soot in Direct Injection Engines," SAE Paper 760129 (1976).

10. Miller, J.A., and Bowman, C.T., "Mechanism and Modeling of Nitrogen Chemistry in Combustion," Progress in Energy and Combustion Science, 15, 287-338 (1989).

11. Foster, D.E., University of Wisconsin-Madison, Department of Mechanical Engineering "An Overview of Zero-Dimensional Thermodynamic Models for IC Engine Data Analysis," SAE Paper 852070 (1985).

12. Ahmad, T., and Plee, S.L., "Application of Flame Temperature Correlations to Emissions from a Direct-Injection Diesel Engine," SAE Paper 831734 (also in SP-557)

13. Amsden, A.A., O'Rourke, P.J. and Butler, T.D., "KIVA-II - A Computer Program for Chemically Reactive Flows with Sprays," Los Alamos National Labs., LA-11560-MS, (1989).

14. Yoshizaki, T., Nishida, K., and Hiroyasu, H., "Approach to Low NO_X and Smoke Emission Engines by Using Phenomenological Simulation," SAE Paper 930612 (1993).

15. Kong, S.C.and Reitz, R.D., "Spray Combustion Processes in Internal Combustion Engines," to be published in Recent Advances in Spray Combustion, Edited by K.K. Kuo, AIAA Series, (1995).

16. Patterson, M., Kong, S.C., Hampson, G., and Reitz, R.D., "Modeling the Effects of Fuel Injection Characteristics on Diesel Engine Soot and NOx Emissions," SAE Paper 940523 (1994).

17. Roblee, L. H. S., Jr., "A Technique for Sampling Reaction Intermediates in a Rapid Compression Machine," Combustion and Flame, 3, pp. 229-234 (1961).

18. Martinengo, A., Melczer, J., and Schlimme, E., "Analytical Investigations of Stable Products During Reaction of Adiabatically Compressed Hydrocarbon Air Mixtures," 10th Symp. (Int.) Combust., The Combustion Institute, pp. 323-330 (1965).

19. Jost, W. and Martinengo, A., "Recent Investigations of Reaction Processes by Means of Adiabatic Compression," SAE Paper 660347 (1966).

20. Moreau, R.A., Sorenson, S.C., and Hull, W.L., "A Technique for Time-Resolved Nitric Oxide Measurements in Auto-Igniting Mixtures," Combustion and Flame, 25, pp. 197-205 (1975).

21. Voiculescu, I.A., "An Experimental Determination of the History of Formation of the Cylinder Averaged Oxides of Nitrogen in Diesel Combustion," Ph.D. Thesis, Department of Mechanical Engineering, University of Wisconsin-Madison (1977).

22. Chan, T.T., "The Effect of Swirl and Exhaust Gas Recirculation on Cylinder Averaged Oxides of Nitrogen Histories in a Diesel Engine," M.S. Thesis, Department of Mechanical Engineering, University of Wisconsin-Madison, (1981).

23. Thien, D.D., "A Further Study of the Dumping Technique as Applied to a Single Cylinder Diesel Engine," M.S. Thesis, Department of Mechanical Engineering, University of Wisconsin-Madison, (1977).

24. Van Gerpen, J.H., "The Effects of Air Swirl and Fuel Injection System Parameters on Diesel Combustion," Ph.D. Thesis, Department of Mechanical Engineering, University of Wisconsin-Madison (1984).

25. Donahue, R.D., "An Experimentally Determined Temporally Based Study of Turbo-Charged Diesel Nitric Oxide Emissions," M.S. Thesis, Department of Mechanical Engineering, University of Wisconsin-Madison, (1993).

26. Chen, S. and Flynn, P., "Development of a Single Cylinder Compression Ignition Engine," SAE Paper 650733 (1965).

27. Chen, S.K., Chang, T.Z., Chang, J.S., and Bair, R., "On-line PC Based Analyzer and Simulator," SAE Paper 881256, (1988).

28. Du, C.J., and Kittelson, D.B., "Total Cylinder Sampling from a Diesel Engine: Part III--Particulate Measurements," SAE Paper 830243 (1983).

29. Shamis, D.A., "The Influence of Fuel Composition on Engine Emissions," M.S. Thesis, Department of Mechanical Engineering, University of Wisconsin-Madison, (1993).

30. Amoco Oil Company, Amofuel LS '94 Diesel Fuel, Amoco Product Information Sheet No. 25.

31. Nikanjam, M., "Development of the First CARB Certified California Alternative Diesel Fuel," SAE Paper 930728 (1993).

32. Krieger, R.B., and Borman, G.L., "The Computation of Apparent Heat Release for Internal Combustion Engines," in Proc. Diesel Gas Power, ASME Paper 66-WA/DGP-4, (1966).

33. Kato, T., Bower, G. and Foster, D., research in progress at ERC, U.W. Madison, to be submitted for SAE 1995 Congress.

34. Yan, J. and Borman G.L., "Analysis and In-cylinder Measurement of Particulate Radiant Emissions and Temperature in a Direct Injection Diesel Engine," SAE Paper 881315 (1988).